

Thermodynamic Parameter of the Martensitic Transformation of NiTi-X-Shape Memory Alloys

V.Prieb (www.materialforschungsservice-dr-prieb.de)
V.Wolff (TU-Berlin, Germany)

Abstract: Polycrystals of NiTi-based shape memory alloys with a third component X (X = Au, Pt, Pd or Al) were examined with calorimetric measurements to investigate the thermodynamic parameters and characteristics of the hysteresis of the thermoinduced martensitic transformation. All known sequences of transformation of NiTi-based shape memory alloys were observed. The enthalpy and entropy of the martensitic transformation B2-R, R-B19' and B2-B19 were measured and calculated. The smallest dissipative characteristics are found for the transformations B2-B19 with invariant plane. The SMART effect in partial thermocycles was investigated and discussed also.

Introduction

The parameters of the transformation hysteresis in shape memory alloys are connected to the dissipation of the elastic energy [1, 2]. The elastic transformation energy arises from incompatibility of lattice at the phase and domain boundaries. This causes stress and rotation moments in the habitus plane, which is relieved by the building of an internal domain structure. This makes the elastic energy of the martensite increase and displace the transformation temperatures out of equilibrium temperature, but minimises the total energy of the two phase system. The energetic state in the habitus plane of martensite changes in TiNi-alloys, when some Ni-atoms are substituted by precious metals Au, Pd and Pt [3]. If the concentration of this elements is about 10at% the $B2 \leftrightarrow B19$ transformation takes place with an crystallographic invariant plane.

It is the aim of this work to show the changes in the sequence of transformation and to investigate the development of thermodynamic transformation parameters and characteristics of hysteresis during the transition to $B2 \leftrightarrow B19$ -

transformation with invariant plane while the composition in shape memory alloys on NiTi-basis is changed.

Experimental Materials and Methods

Three NiTi-Pt-alloys with a Pt-concentration in the critical range about 10 at%Pt were chosen (Table 1). From NiTi-Au and NiTi-Pd alloys only those with an Au- and Pd-concentration of 10% were investigated. They show a change of transformation type from

Table 1. Composition (at.%), type of transformation and characteristic transformation temperatures ($^{\circ}\text{C}$) of the investigated alloys

No.: Type of transformation*	Ti	Ni	Pt	Au	Pd	Al	M_s	M_f	T_p^c	A_s	A_f	T_p^h	T_0, K
1: $B2 \leftrightarrow B19'$	50.0	50.0	--	--	--	--	60.0	44.0	50.0	86.0	99.5	95.0	346.0
2: $B2 \leftrightarrow B19 \leftrightarrow B19'$	50.0	43.0	6.5	--	--	--	50.5 48.0 (55)	(45) (25) 17.0	48.0 (42) (46)	(60) (48) 29.0	63.5 (62) (72)	63.0 (61) (46)	321.0
3: $B2 \leftrightarrow B19$ (i)	50.0	42.1	7.9	--	--	--	7.0	-1.0	5.0	12.5	17.5	16.0	282.0
4: $B2 \leftrightarrow B19$	50.0	34.7	15.3	--	--	--	116.0	104.0	111.0	124.0	131.0	129.5	392.0
5: $B2 \leftrightarrow B19 \leftrightarrow B19'$ (i)	50.0	40.0		10.0	--	--	80.0 76.0 46.0	75.0 70.0 19.0	78.5 73.5 36.0	86.0 83.0 46.0	89.0 88.0 59.0	88.0 85.5 54.0	352.5
6: $B2 \leftrightarrow B19$ (i)	50.0	40.0	--	--	10.0	--	23.0	15.0	18.0	24.0	30.0	28.5	296.5
7: $B2 \leftrightarrow R$ $R \leftrightarrow B19'$	48.2	50.0	--	--		1.8	22.0 -75.0	15.0 -97.0	19.0 -82.0	23.0 -29.0	31.0 -15.0	29.0 -19.0	295.5 221.0

*results from X-ray diffraction

$B2 \leftrightarrow B19'$ to $B2 \leftrightarrow B19$ with invariant plane. The alloy of two components NiTi with $B2 \leftrightarrow B19'$ -transformation was investigated as basic alloy with the same measurements. The addition of aluminium allows to separate $B2 \leftrightarrow R$ - and $R \leftrightarrow B19'$ -transformations clearly [3], so that the parameters of transformation can be determined more precise as in [4] for each of them.

The polycrystal samples of the investigated alloy were annealed at 1100 K for 30 minutes, quenched in water and etched. At last the samples were tempered just in the calorimeter at 700 K before the calorimetric measurements.

The transformations $B2 \leftrightarrow B19$ with invariant plane¹ are signed by an index i . The calorimetric measurements were carried out in a calorimeter DSC-7 Perkin Elmer PC-series with a scanning rate of 4 K/min. The utilisation of the calorimetric curves as well as the definitions and the calculation of the thermodynamic parameters and the characteristics of hysteresis are described in [1, 4]. The temperatures T_p^c , T_p^h denote the temperatures of the peaks in the calorimetric curves during cooling and heating (Table 1).

Experimental Results

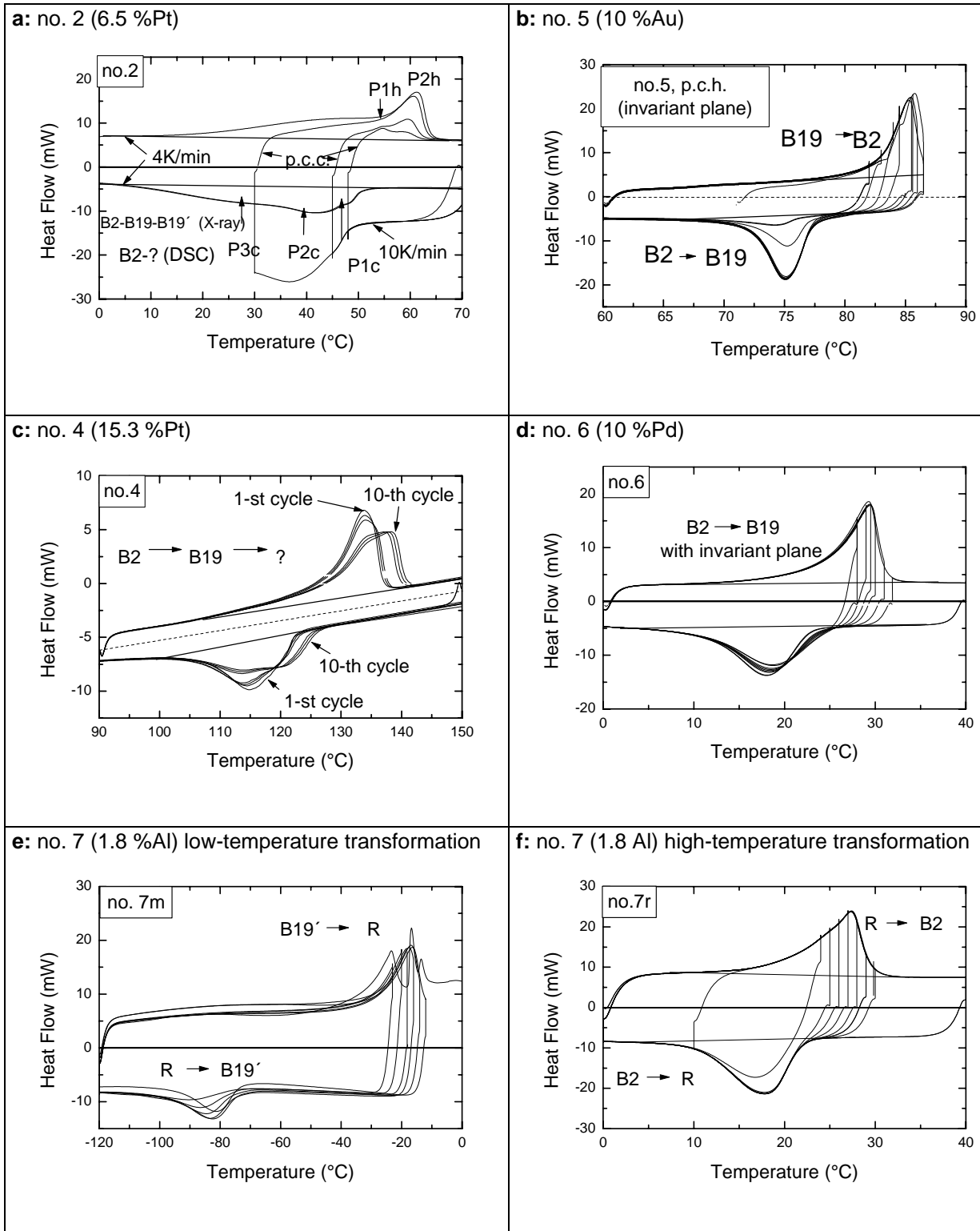
Sample 1 is characterised by calorimetric curves (CC) with one single peak corresponding to transformation $B2 \leftrightarrow B19'$. If the forward transformation is interrupted in partial cycles, first the CC-peaks show an asymmetry while heating and then with decreasing fraction of martensite reached in forward transformation two not completely resolved peaks. The second peak corresponds to the transformation $R \rightarrow B2$. If the reverse transformation is interrupted at lower and lower temperatures (the SMART-procedure [2]), the original peak separates in three peaks divided clearly by deep minima at the next complete reverse transformation like the $B19' \rightarrow R$ -SMART of sample 7 (fig. 1e). It was observed an evident SMART effect, though the temperatures of the three peaks have no visible correspondence with the temperatures of interrupt in the partial cycles.

The transformations in the samples 3, 4 and 6 are characterised through the single CC peaks. The peaks are asymmetric, because they are extended to lower temperatures at the forward as well as at the reverse transformation (fig. 1b, d). The peak for sample 4 becomes asymmetric at the complete transformation cycles and

¹ The samples and the results of X-ray diffraction were kindly placed at our disposal by Dr. V.P. Sivocha (Tomsk, Russia).

after ten cycles it has become a slightly resolved twin peak (fig. 1c). The widening of the peak is caused by the increasing temperature of the high temperature transformation, while the temperature of the second transformation not changes.

Fig.1(a-f). DSC-Diagramms for samples:



An evident SMART effect exists for the transformation of sample 4 with the slightly resolved CC peak also. The transformation of sample 5 is characterised through three CC peaks (fig. 1b): The main peak with the highest intensity was accompanied by two satellite peaks at higher and lower temperatures (Table 1). At the partial SMART cycles the SMART effect is observed at the left shoulder of the peaks of sample 3 and of the main peak of sample 5 all being enlarged to lower temperatures, but the turning points at higher temperatures have no effect on the right shoulder of the peak (fig. 1b). Also there is no recognisable connection between the irregularities of the SMART peaks and the temperatures of the turning point. The SMART effect is very small in both samples. The sample 6 doesn't show any SMART effect (fig. 1d).

Table 2. Thermodynamical transformation parameters and hysteresis characteristics

No	$\left \frac{\Delta T^{AM}}{\Delta T^{MA}} \right , K$	$\Delta T, K$	$\Delta T', K$	$\left q^{AM} / q^{MA} \right , J / g(!)$	$\left \Delta s^{AM} / \Delta s^{MA} \right , J / kg \cdot K$	$\left \Delta \bar{s} / \Delta s' / \Delta s_0 \right , J / kg \cdot K$	$\left k_T^{AM} / k_T^{MA} \right , J / kg$	$\varepsilon_D, J / g(!)$	$\varepsilon'_D, J / g(!)$
1	16.0/13.5	40.8	26.0	27,7/27,9	85.6/75.8	80.7/80.3/81.6	650.4/548.8	3.3	2.1
2	(23)/(34)	15.0	0	11,4/14,2	36.2/42.5	39.4/39.9/39.0	(662)/(682)	0.6	0
3i	8.0/ 7.5	11.0	4.0	6,0/ 7,6	21.6/26.2	23.9/24.1/23.8	98.0/ 91.9	0.3	0.1
4	10.0/ 7.0	18.0	10.0	11,0/12,2	28.2/29.9	29.1/29.6/29.3	120.5/ 84.4	0.4	0.2
5i	6.0/ 6.0	11.0	5.0	7,9/ 8,3	22.8/23.2	23.0/23.0/22.8	63.9/ 63.9	0.2	0.1
6i	8.0/ 9.0	11.0	1.0	7,9/ 9,3	27.1/30.8	29.0/29.0/28.7	112.0/ 84.0	0.3	0.1
7r	7.0/ 8.0	8.5	1.0	7,0/ 7,4	23.9/24.5	24.2/24.4/24.0	85.4/ 97.6	0.2	0
m	22.0/14.0	64.0	46.0	5,2/ 7,4	27.2/29.1	28.2/28.5/27.6	313.5/199.5	1.8	1,3

In Table 1: $\Delta s^{AM,MA} = q^{AM,MA} / T_p^{c,h}$; $\Delta \bar{s} = (\Delta s^{AM} + \Delta s^{MA}) / 2$; $\Delta s' = (q^{AM} + q^{MA}) / T'_0$ (T'_0 accordingly [1]); $\Delta s_0 = (q^{AM} + q^{MA}) / T_0$ (T_0 accordingly Tong and Wayman); $\Delta T^{AM}, \Delta T^{MA}$ - interval of temperature of the forward and reverse transformation, $\Delta T' = A'_s - M'_s$ - width of the latent hysteresis and ε'_D - the dissipated energy corresponding to the latent hysteresis [1]

Discussion

The experimental data show, that all possible transformations in TiNi-based alloys have very different characteristics of transformation and parameters of hysteresis. The $B2(R) \leftrightarrow B19'$ transformation of the stoichiometric NiTi alloy (sample 1) has the highest values of enthalpy and entropy and a wide hysteresis, what causes

the highest dissipation of energy. The $R \leftrightarrow B19'$ transformation shows the widest hysteresis, although the transformation enthalpy and entropy are much lower than the values of sample 1 and more like the values of the $B2 \leftrightarrow B19$ transformation in the samples 3-6 and the $B2 \leftrightarrow R$ transformation of sample 7. Transformation $B2 \leftrightarrow R$ as well as transformation $B2 \leftrightarrow B19$ with invariant plane are accompanied by very small dissipation. Such dissipative characteristics and similar values of entropy are known from Cu-based single crystals and the stoichiometric NiTi single crystal [1, 2]. One can conclude from this results, that the SMART effect is correlated with the dissipation of the elastic energy and has the same mechanism.

As shown in table 2, the transformation entropy doesn't depend on the composition of the alloy but on the softening of the elastic modules [3] respectively on the anomalies of the phonon spectrum. Concerning the method the specific values of entropy (per mass unit) depend on the completeness of transformation [1]. This is the reason for the differences in the entropy for transformations with invariant plane. The asymmetry and dissolving of the KK peaks of the samples 2 and 4 could be connected to the $B2 \leftrightarrow R \leftrightarrow B19'$ transformation for neither the number of KK peaks nor their intensity correspond to the sequence of transformation $B2 \leftrightarrow B19 \leftrightarrow B19'$ which is found by X-ray measurements. Only the twin peak of sample 4 dissolved after some cycles could correspond to this transformations, but this would mean that both happens at the same time not sequential. The calorimetry is not a method to analyse phases directly, but it is more sensitive than X-ray measurements, and if the values of entropy are known, it can be used for the analysis of the completeness of the transformation [1].

Literature:

1. Prieb V., Link T., Feller-Kniepmeier M., Steckmann H. et al. Influence of the Structure and Orientation of the Parent Phase on the Hysteresis of Single-Crystal Shape Memory Alloys. //J. de Physique IV, Colloque C8 (ICOMAT'95)., 5(1995)913-918.
2. Prieb V., Steckmann H. Thermoelasticity and hysteresis of martensitic transformation in shape memory alloys. Parts I-III. //Tech. Phys., 41(1996)1132-1144.
3. Khachin V.N., Voronin V.P., Sivokha V.P. and Pushin V.G. Martensitic Transformation and Shape Memory Effect in Polycomponent TiNi-Based Alloys. // J. de Physique IV, Colloque C8 (ICOMAT'95)., 5(1995)707-712
4. Prieb V. and Steckmann H. Thermoelasticity and hysteresis of martensitic transformations in shape memory alloys. I. Hysteresis of the stress-free thermal transformation.//Tech. Phys., 41(1996)1132-1136